Detecting Axions

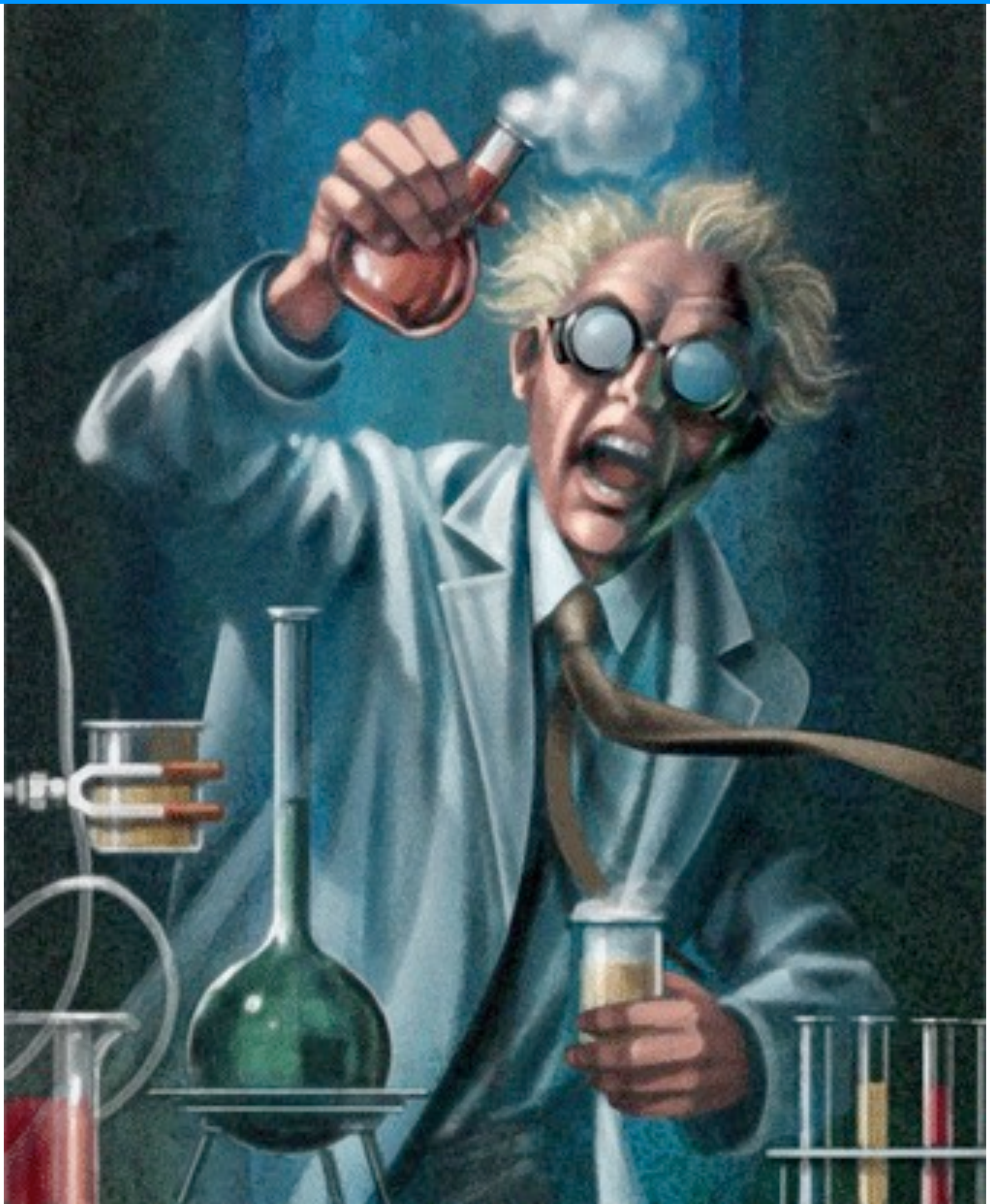

$$\rho_{\mathrm{aDM}} = 0.3 \frac{\mathrm{GeV}}{\mathrm{cm}^3}$$

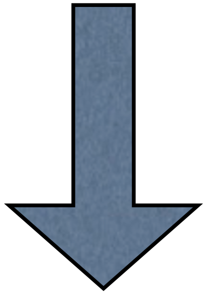

$$\theta_0 = 3.6 \times 10^{-19}$$

How to search for “invisible” WISPs

> Axion and axion-like particles: exploit the coupling to photons.

> photon + photon ↔ ALP
photon + ALP → photon

> photon + (virtual photon) → ALP
ALP + (virtual photon) → photon

A virtual photon can be provided by an electromagnetic field.

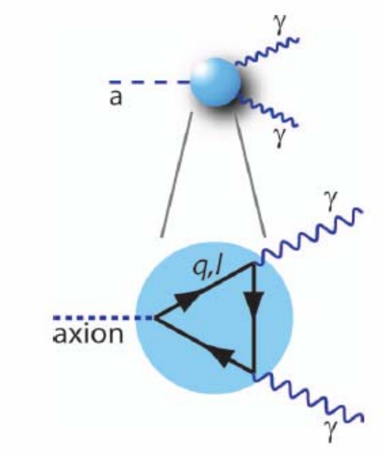

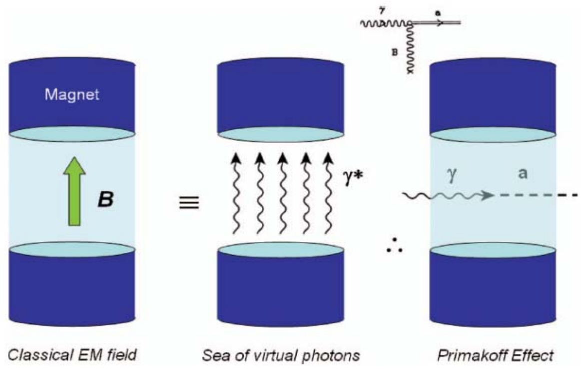

The Search for Axions,
Carosi, van Bibber, Pivovaroff,
Contemp. Phys. 49, No. 4, 2008

WISP = Weakling Interacting Slim Particles

Axion experiments 2017

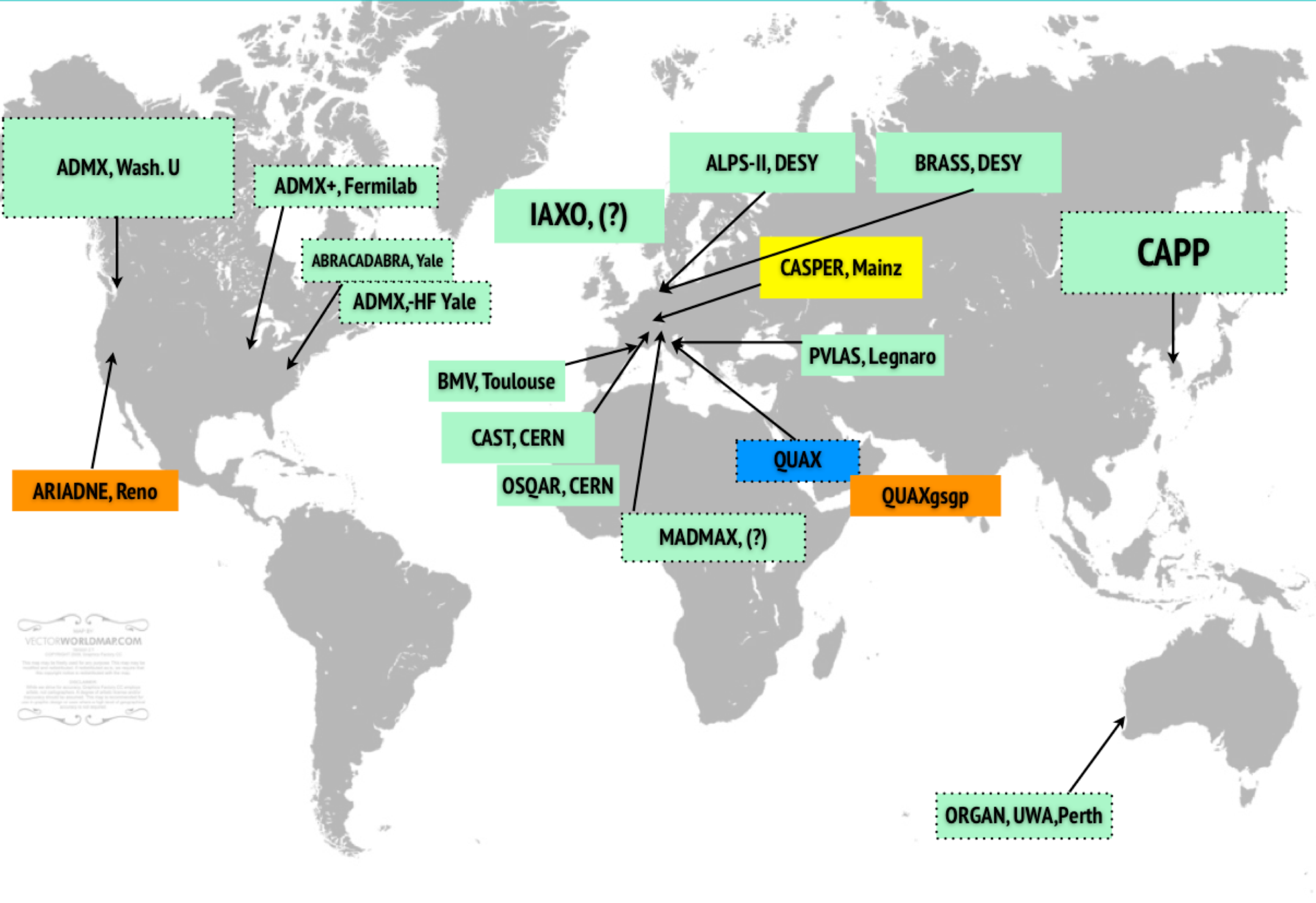

Axions Experiments

3 classes of experiments: Haloscopic, Helioscopic, Laboratory (LSW)

$m_a < 3\times10^{-3}$ eV from SN1987

Axion, like neutral pion couples to two photons via Primakoff effect)
Detected in a magnetic field H

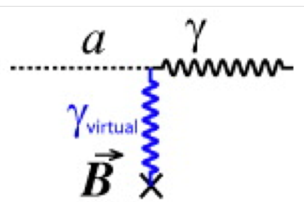

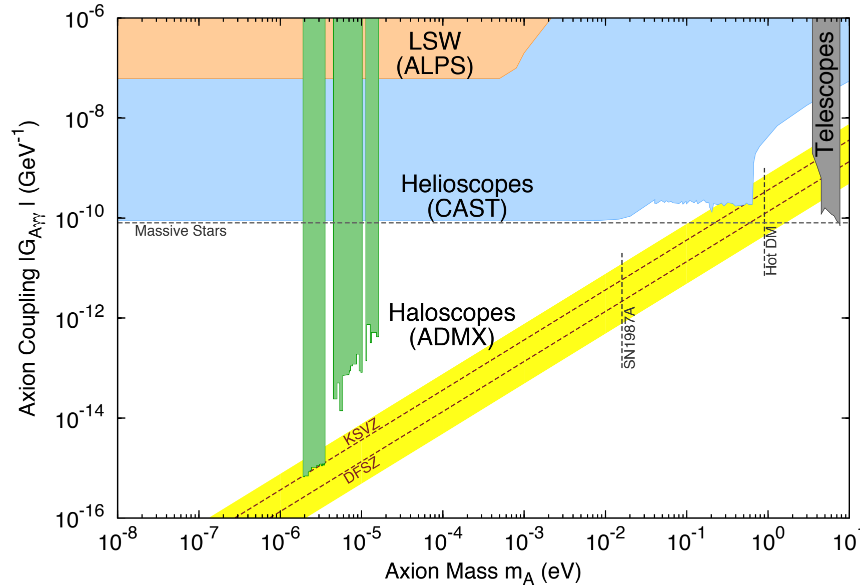

Yellow band represent theoretical predictions from DFSZ and KSVZ axion models

Haloscopic: cavity like ADMX
Are the only experiments hitting
the Peccei-Quin region (QCD axions)

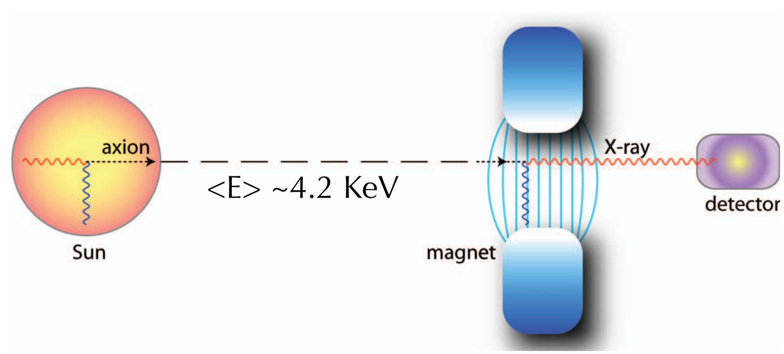

Helioscopic: depend on stellar models
CAST (best limit at the moment) and
IAXO (next CERN exp.) use LHC dipoles

ADMX – Seattle - USA

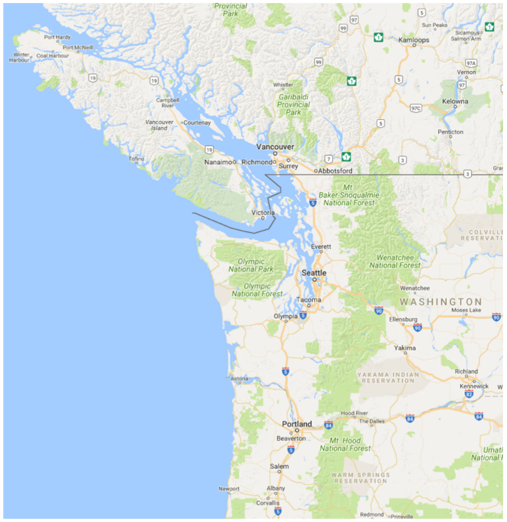

Haloscopic: axions from intergalactic Halo

Cavity: in the strong magnetic field axion converts to a photon with the same energy

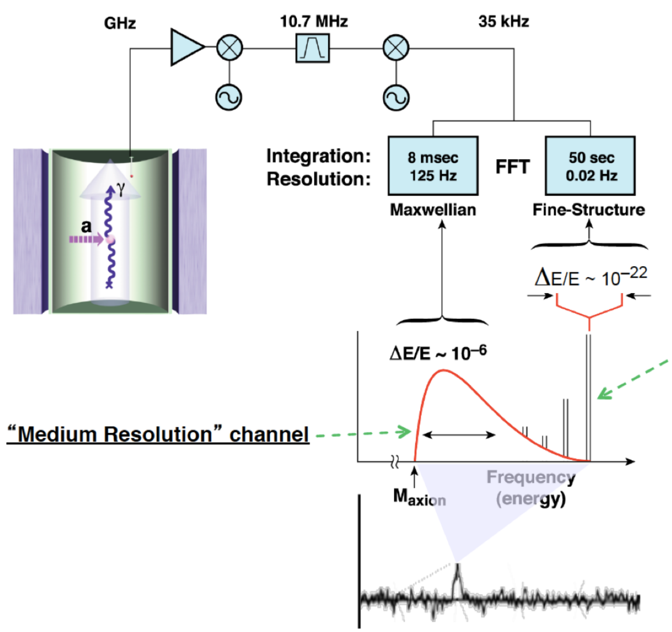

Haloscopic Experiment in Cavity

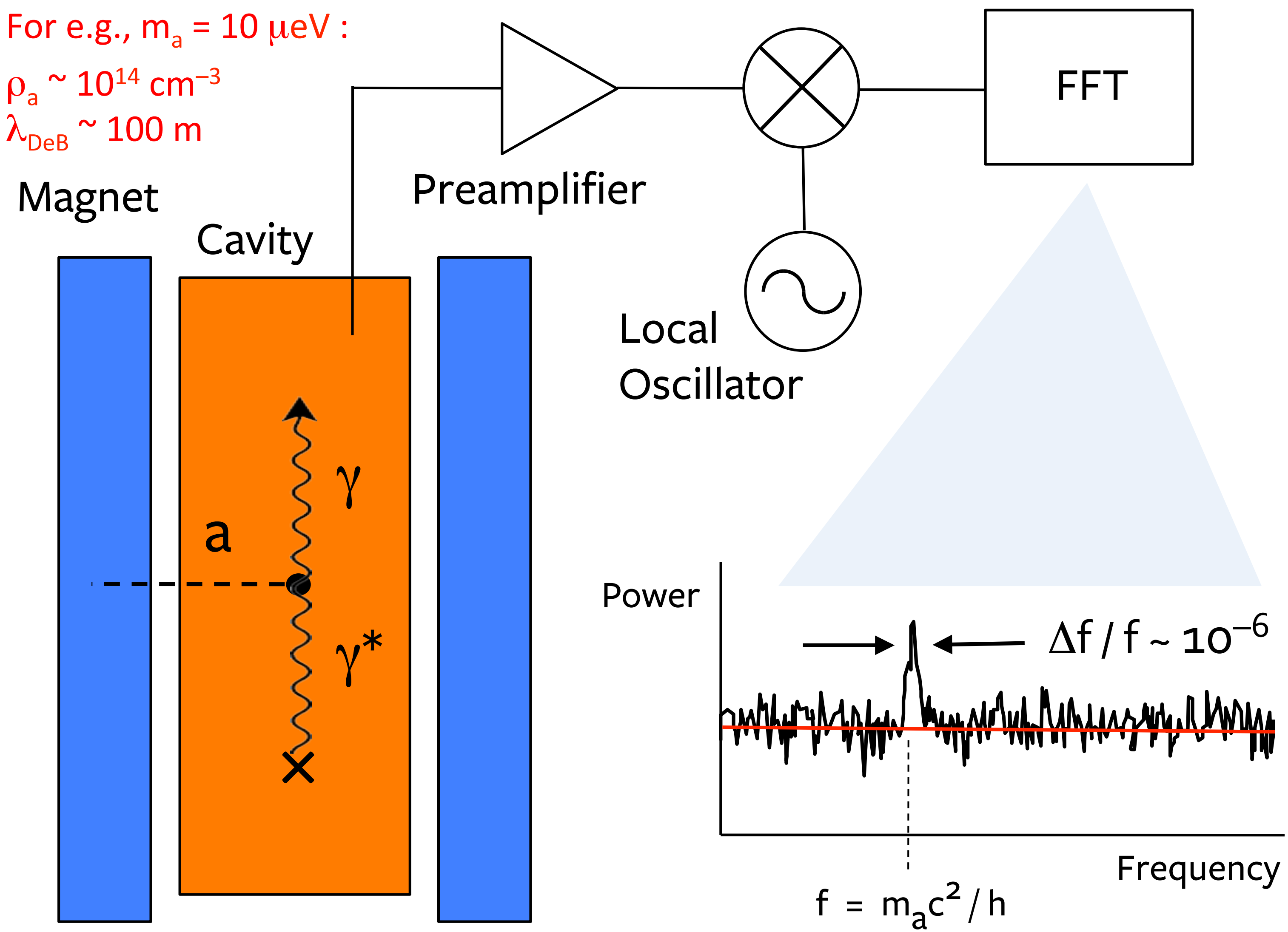

S/N and Detectability

HAYSTAC

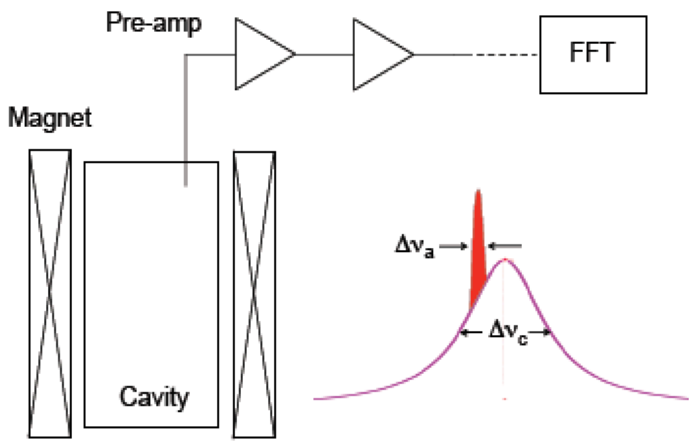

Cavity Bandwidth: $\Delta\nu_c / \nu_c = Q^{-1} \sim 10^{-4}$

Axion Bandwidth: $\Delta\nu_a / \nu_a \sim \beta^2 \sim 10^{-6}$

- Naive ADMX scaling (e.g. an ADMX every octave)

- Signal $(V \propto m_a^{-3})$ $\quad P_{\rm out} \propto V m_a \sim \frac{1}{m_a^2}$

- Noise $P_{\rm noise} = T_{\rm sys} \Delta\nu_a \propto m_a^2$

- Signal/noise in $\Delta\nu_a$ of time, t, $\frac{S}{N} = \frac{P_{\rm out}}{P_{\rm noise}} \sqrt{\Delta\nu_a t}$

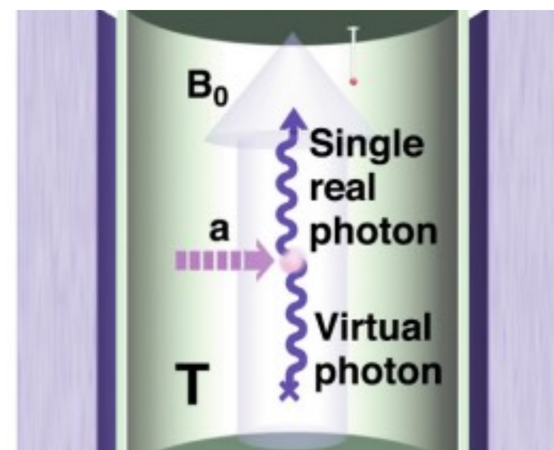

Note $T_S \approx T + T_A$, *for* $T >> h\nu$

TA = amplifier temperature, noise temperature equivalent of receiver antenna (or amplifier)

ADMX –USA

superconducting quantum interference device

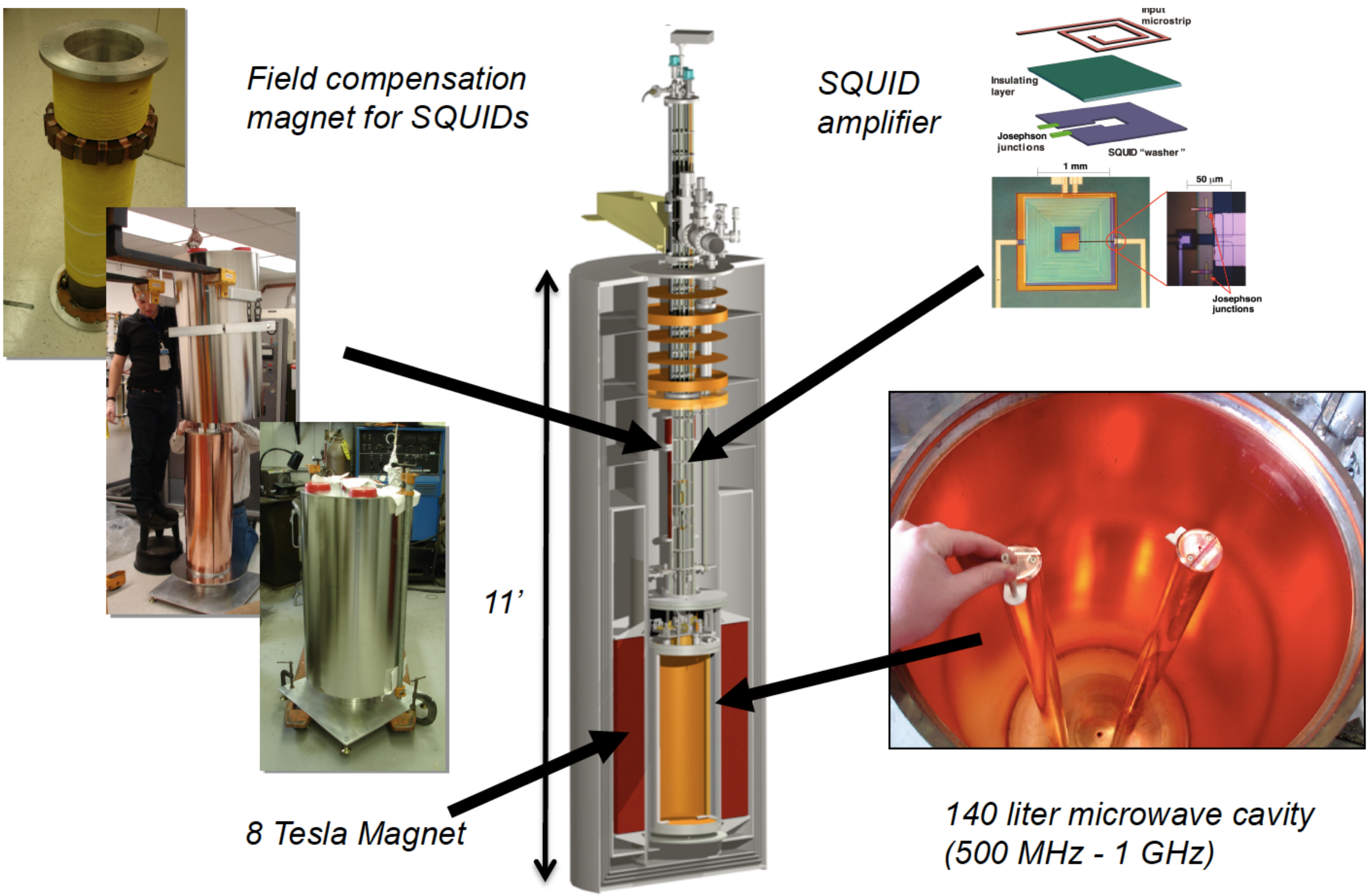

Microwave Cavity needs tunable resonance

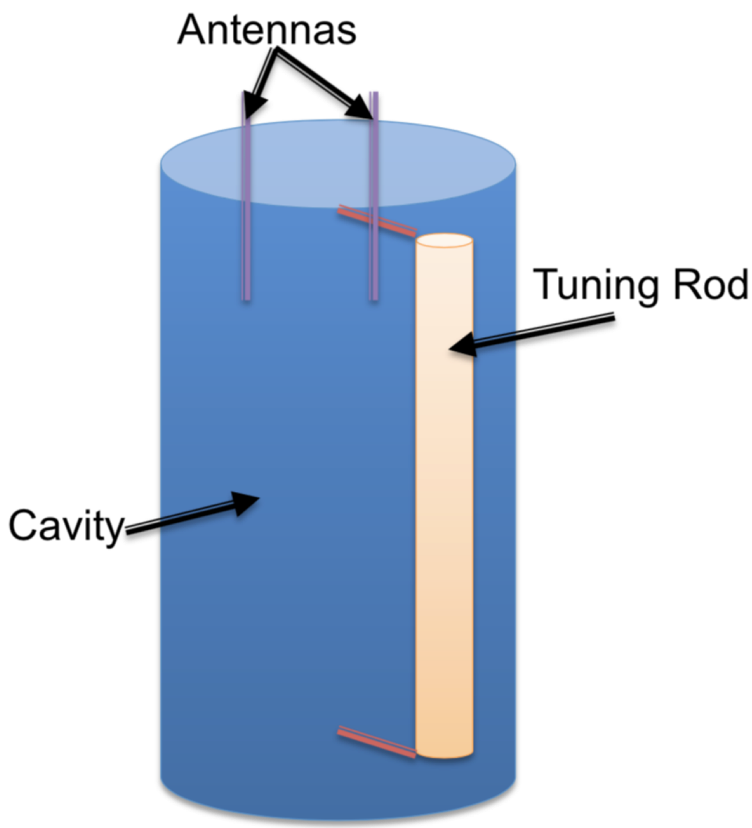

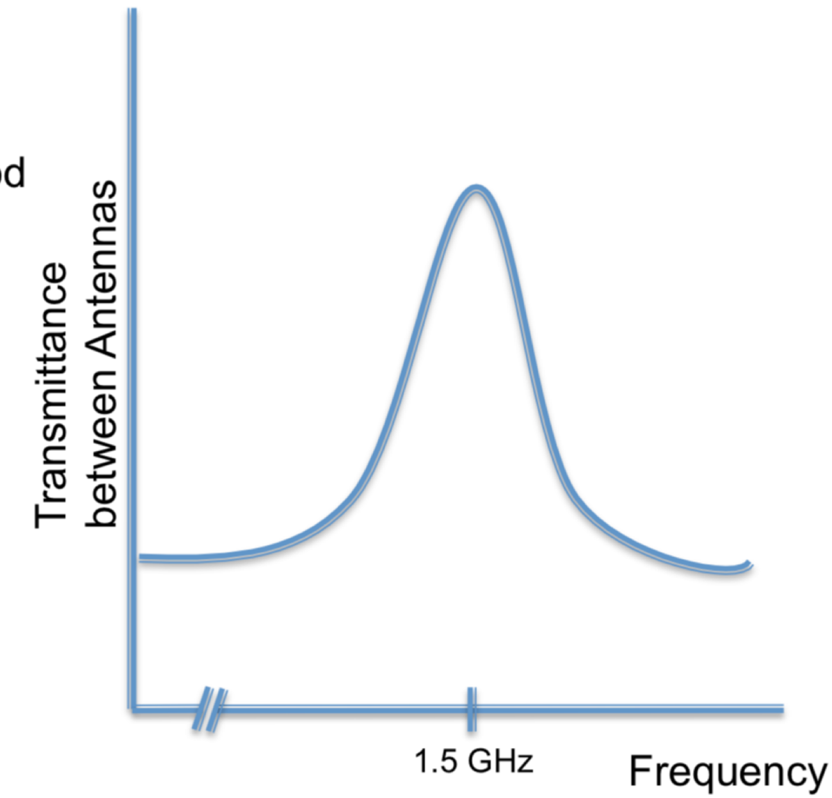

Scanning over frequencies

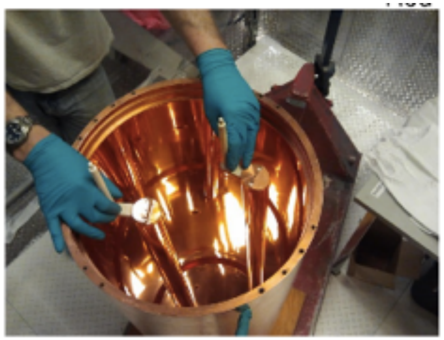

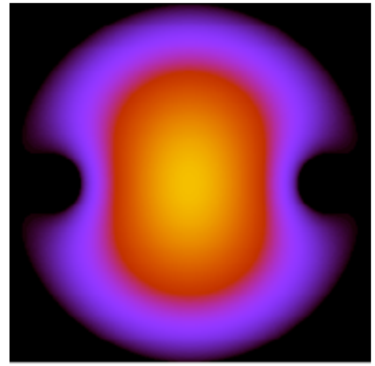

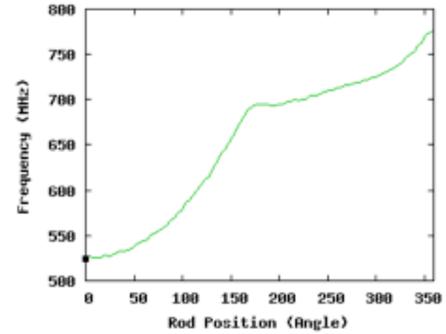

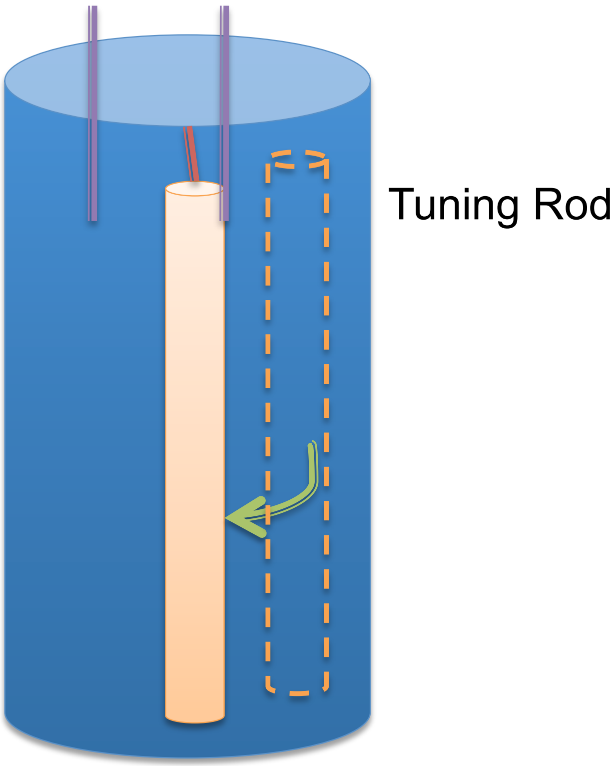

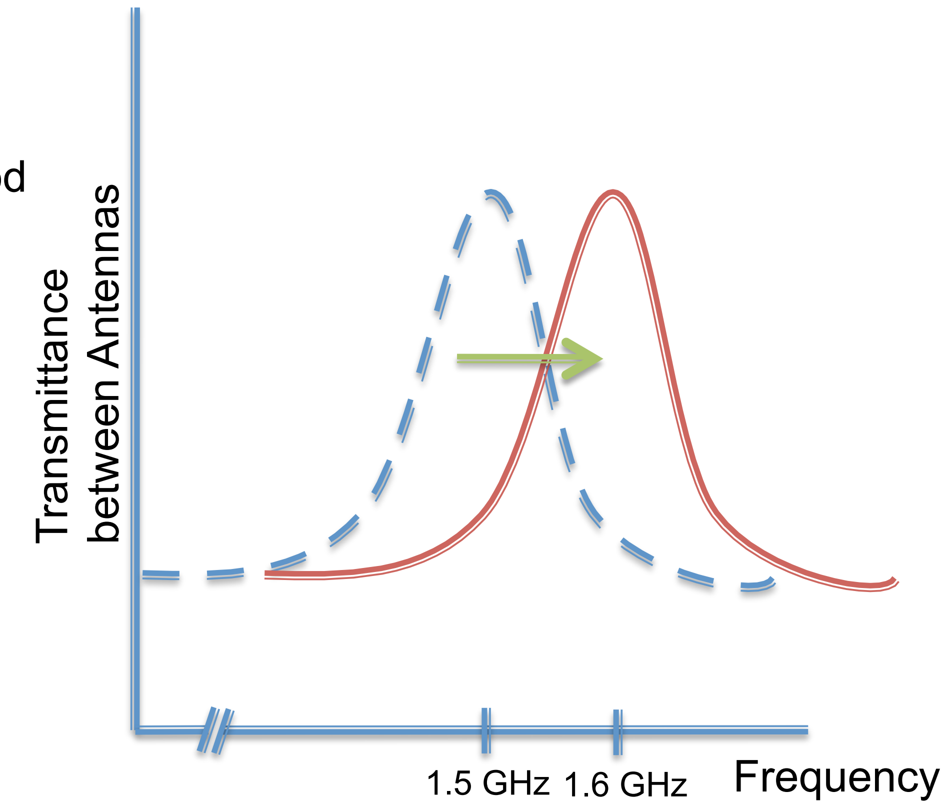

Quantum Amplifiers

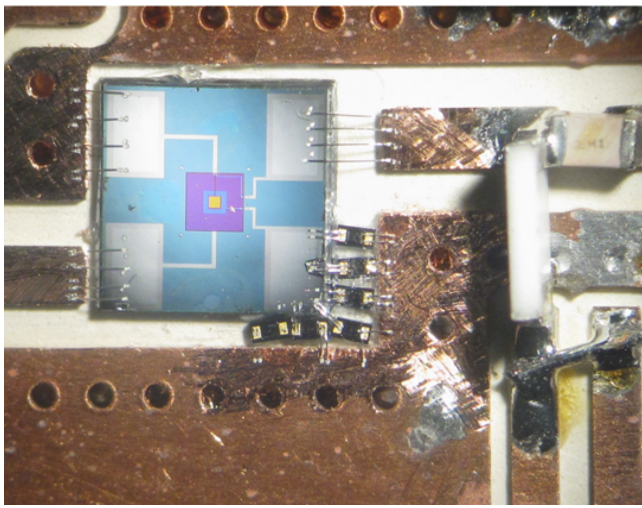

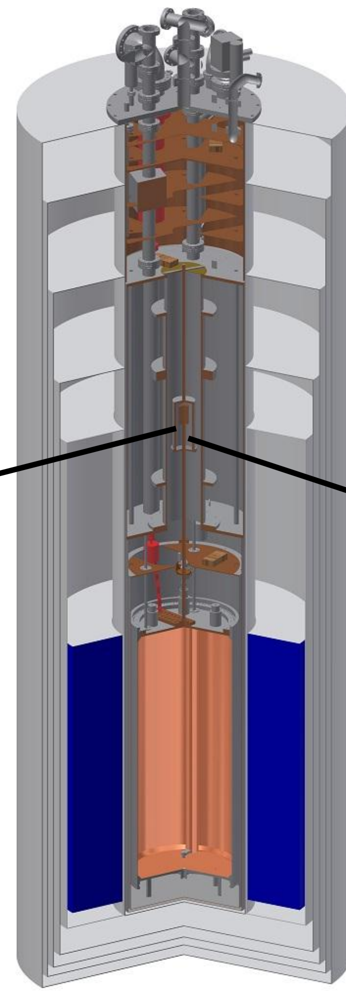

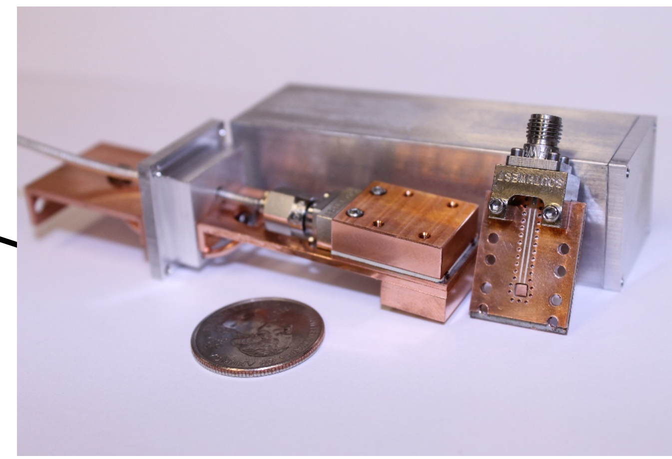

SQUIDs
(at lower frequencies)

“JPAs”
(at higher frequencies)

Raw data and hardware synthetic axion (×100)

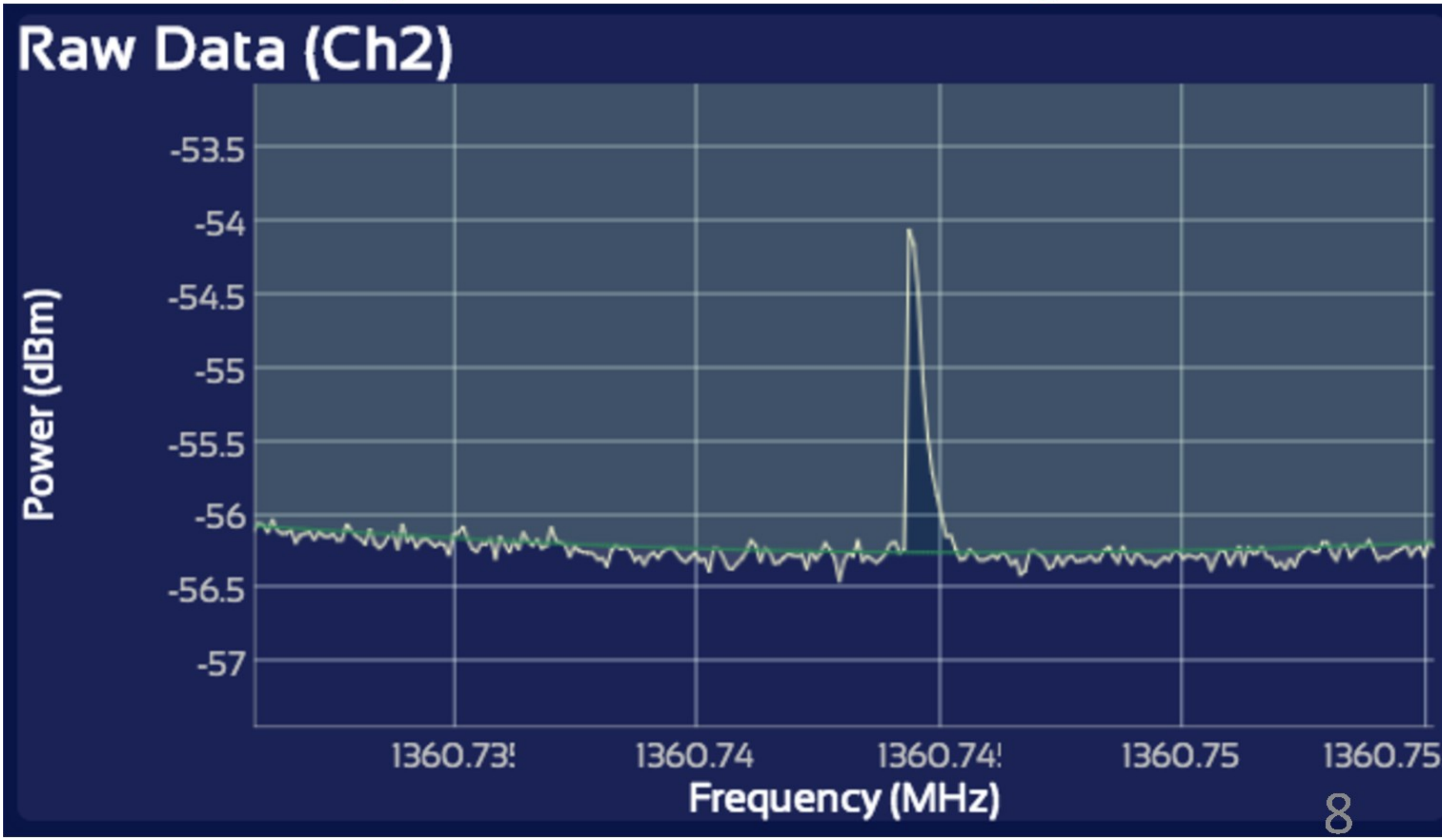

ADMX Gen 2 Science Prospects: Year 1 (0.5 – 1 GHz)

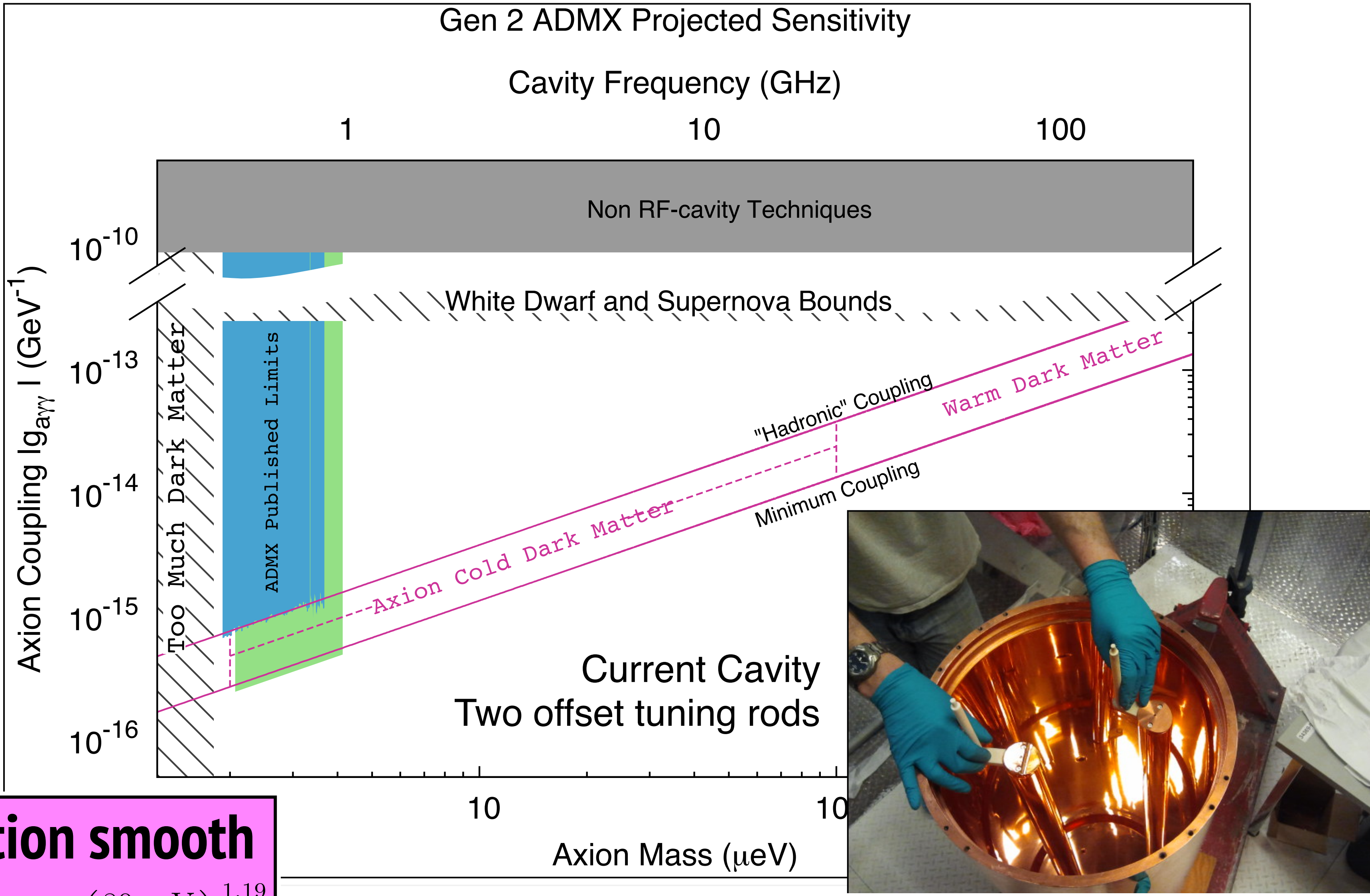

Inflation smooth

$$\Omega_{\mathrm{aDM}} h^2 \simeq \theta_I^2 \left(\frac{80\,\mu\mathrm{eV}}{m_a} \right)^{1.19}$$

CAST – CERN – Geneva, CH

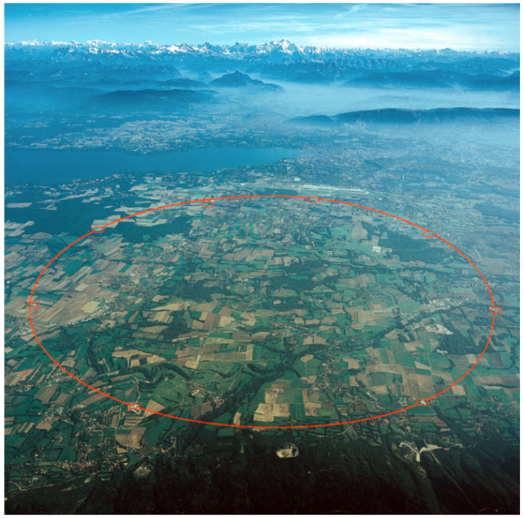

LHC dipole: 9 Tesla magnet pointing to the Sun

Sensitivity: important experimental sensitivity to axion-photo coupling but depends on stellar models

Magnet can move ±8° vertically and ±40° horizontally (1h30 sunset/sunrise)

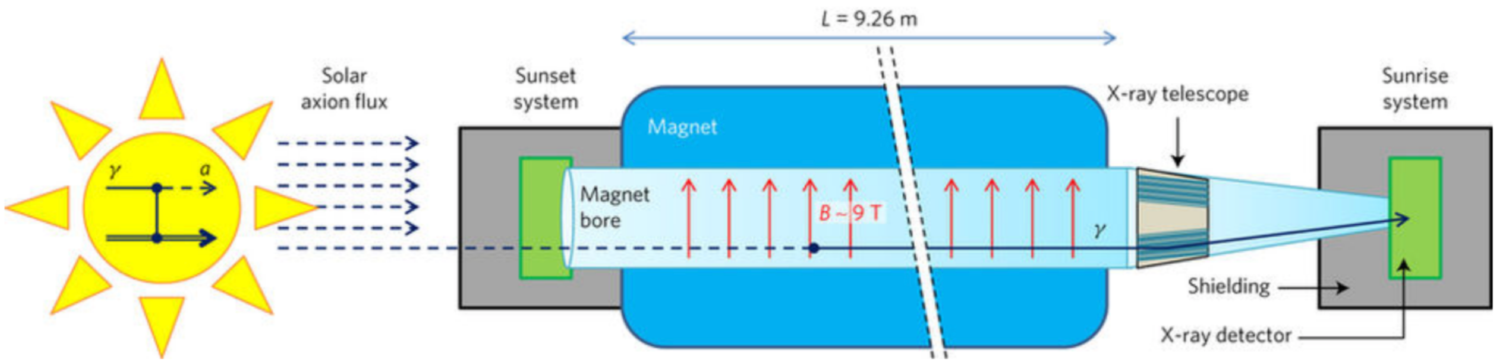

Axions produced in the Sun by Primakoff scattering and converted back to X-rays by the same process in the B field of an LHC magnet

2 different detectors at the 2 magnet sides

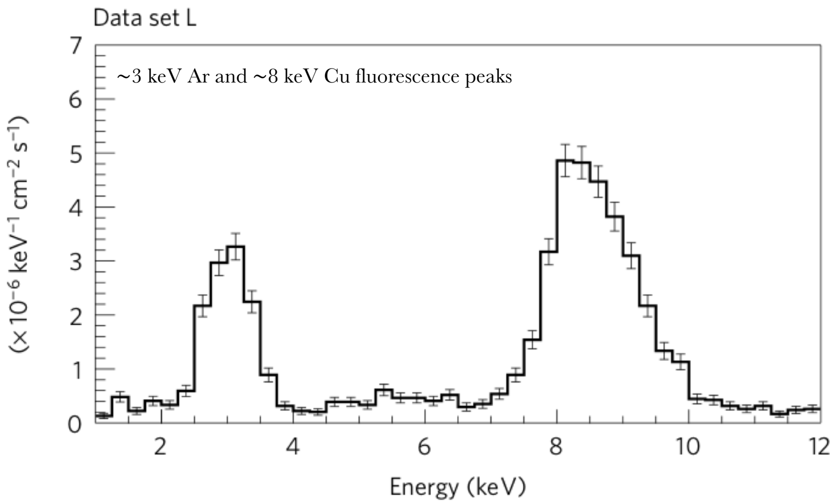

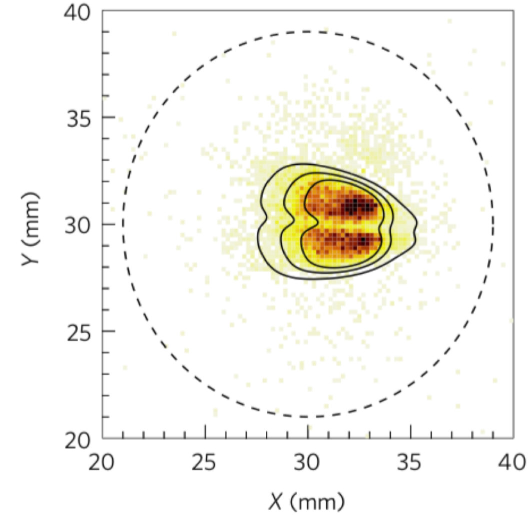

Table 1 | Tracking and background exposure, as well as the integrated 2–7 keV measured count rate, for both tracking and background data, for each of the data sets included in our result.

Data set	Detector	Year	Tracking exposure (h)	Background exposure (h)	Measured count rates (±1σ error) (10^{-6} keV^{-1} cm^{-2} s^{-1})	
					Tracking	Background
A	SS1	2013	92.5	1,700.0	0.79±0.18	0.81±0.04
B	SS2	2013	86.5	1,407.8	1.37±0.24	1.48±0.06
C	SS1	2014	118.0	1,854.0	0.94±0.17	1.03±0.05
D	SS2	2014	118.1	1,819.6	0.97±0.18	1.05±0.05
E	SS1	2015	79.5	1,237.6	0.77±0.18	0.89±0.05
F	SS1	2015	49.7	783.1	1.77±0.36	1.65±0.09
G	SS1	2015	83.5	1,431.5	1.32±0.25	1.10±0.05
H	SS2	2015	81.3	1,236.2	0.70±0.18	0.89±0.05
I	SS2	2015	51.3	800.2	1.04±0.27	1.59±0.08
J	SS2	2015	82.0	1,409.2	0.91±0.20	0.90±0.05
K	SR	2014	69.8	1,379.4	0 counts	0.25±0.05 counts
L	SR	2015	220.4	4,125.4	3 counts	0.77±0.15 counts
Total tracking exposure (h):			1,132.6			

Note that for rows K and L background levels are expressed in units of total counts in the (95% signal-enclosing) spot area during the corresponding tracking exposure.

$$P_{a\to\gamma} = \left(g_{a\gamma} B \frac{\sin(qL/2)}{q} \right)^2$$

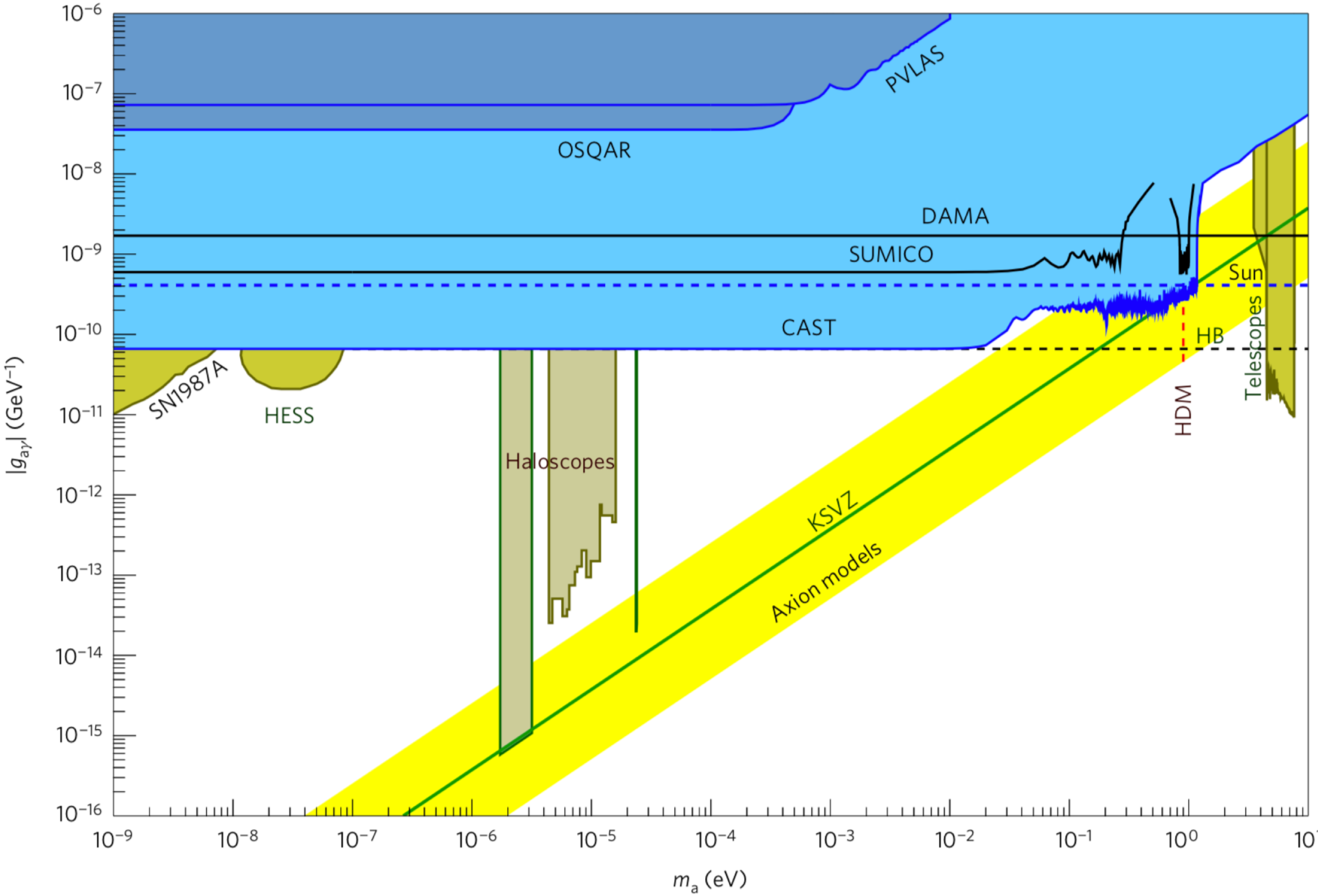

Many different detectors used for this experiment in the years

multiwire time projection chamber, Micromegas detectors, low-noise charged coupled device attached to a spare X-ray telescope (XRT) from the ABRIXAS X-ray mission, a **γ-**ray calorimeter, and a silicon drift detector

Ready for next generation axions helioscope: **IAXO**

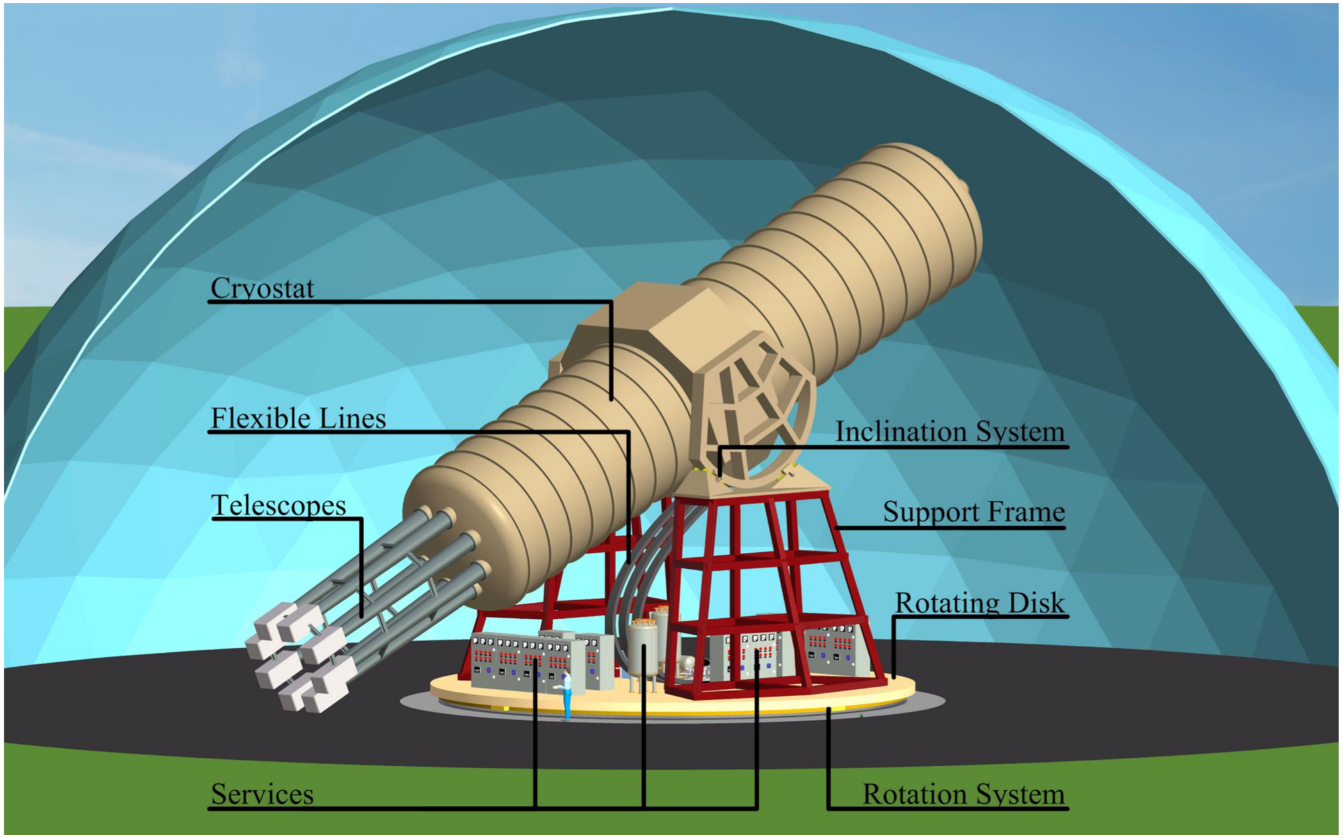

Light Shining through a Wall Experiments

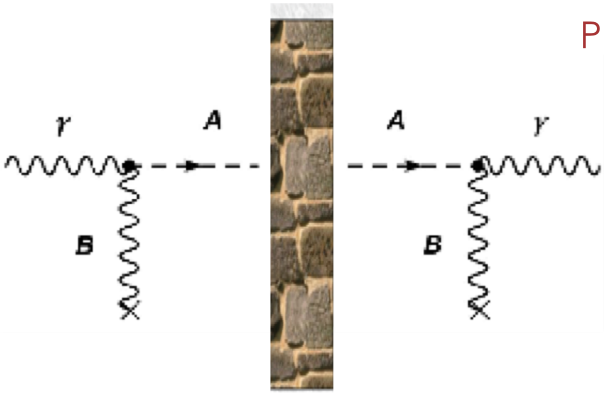

P. Sikivie, Phys. Rev. Lett. **51**, 1415 (1983)

LAB experiment
Laser Source
Higher Luminosity

Double process
Rate ~ G^4

$$\dot{N}_{\text{evts}} \propto \dot{N}_\gamma \, P_{\gamma \to a} \times P_{a \to \gamma} \sim \dot{N}_\gamma \, G^4 H^4 L^4$$

Sensitivity on G linear with L and H, quartic root of luminosity (not depending on E_γ)

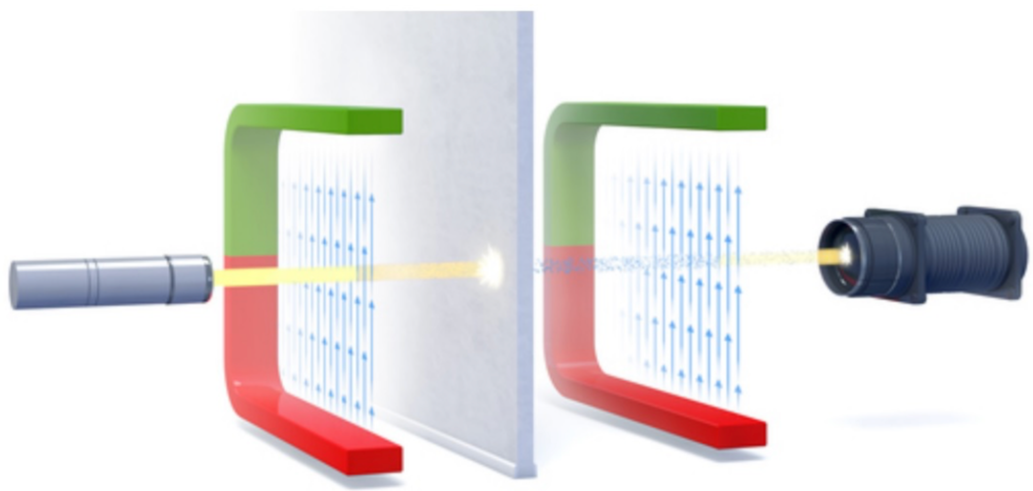

Axion Production in a magnetic Field

- The production (and re-conversion) of WISPs takes place in a coherent fashion.

  For ALPs (Φ):

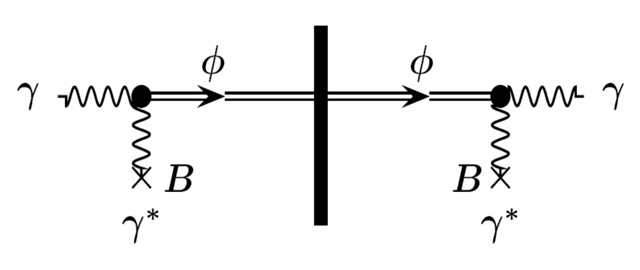

$$P_{\gamma\to\phi}(B,\ell,q) = \frac{1}{4}\,(g\,B\,\ell)^2\;F(q\ell) \qquad F(q\ell) = \left[\frac{\sin\left(\frac{1}{2}q\ell\right)}{\frac{1}{2}q\ell}\right]^2$$

q = $p_\gamma - p_\Phi$
l: length of B field

$g = (P)^{1/4} \cdot 2 \cdot / (l \cdot B) / F^{1/2}$

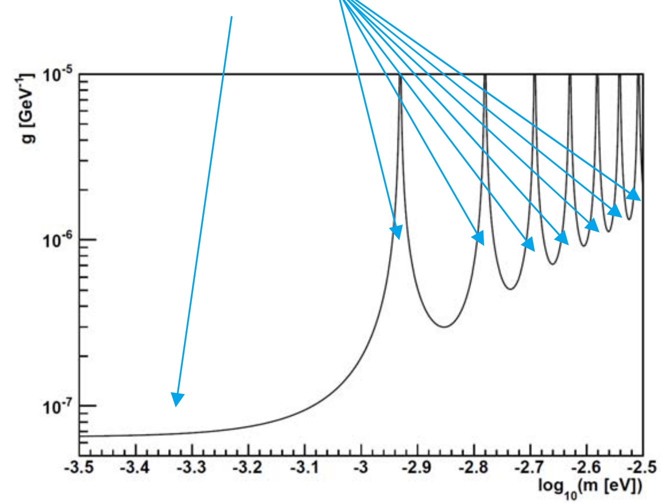

The ALPS Project

Any Light Particle Search @ DESY

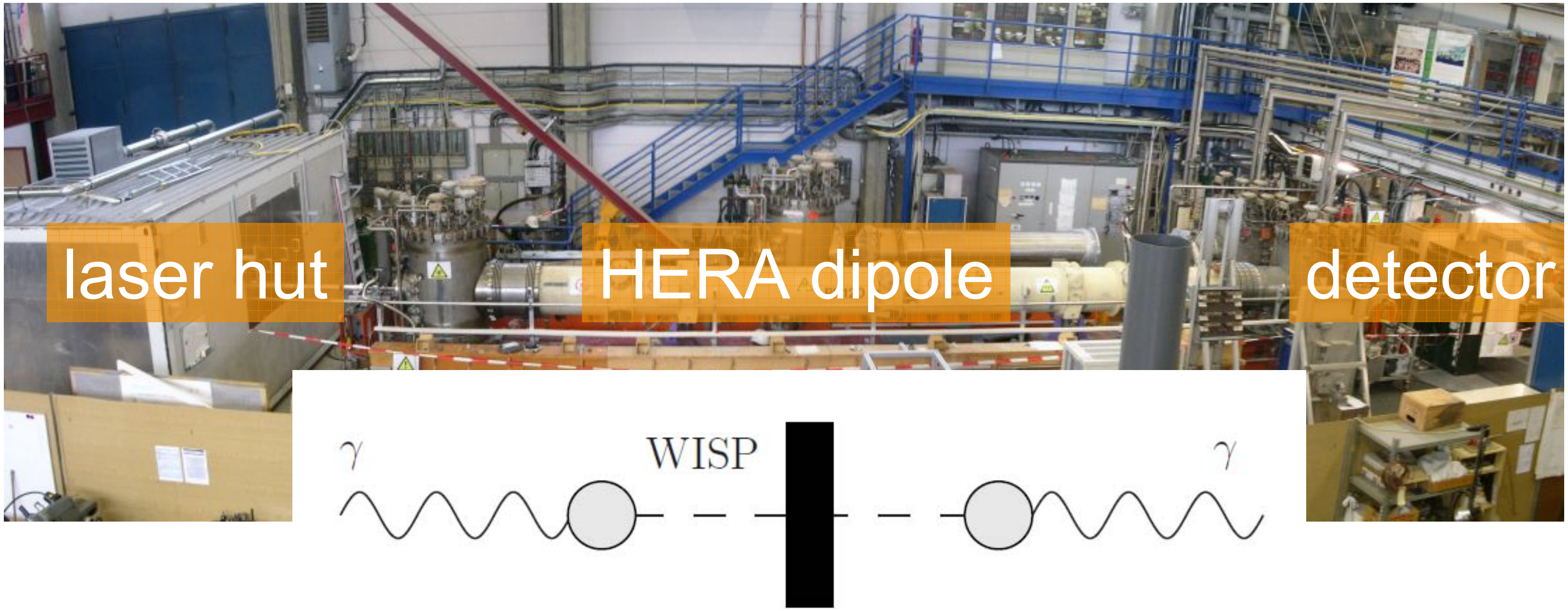

A "light-shining-through-a-wall" experiment

Three main ALPS Components

- Powerful laser:
  optical cavity to recycle laser power
  (high quality laser beam)

- Strong magnet:
  HERA dipole: 5 T, superconducting
  (unfortunately just one)

- Sensitive detector:
  CCD
  (determines wavelength of laser light!)

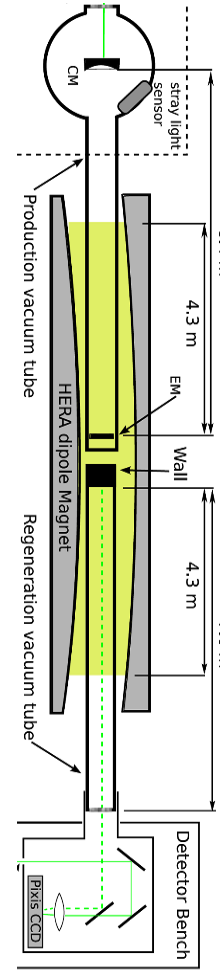

Tubes:
- diameter: 34 mm
- clear aperture: 14 mm

Charge coupling device

ALPS Results:

(PLB Vol. 689 (2010), 149, or http://arxiv.org/abs/1004.1313)

- Unfortunately, no light is shining through the wall!

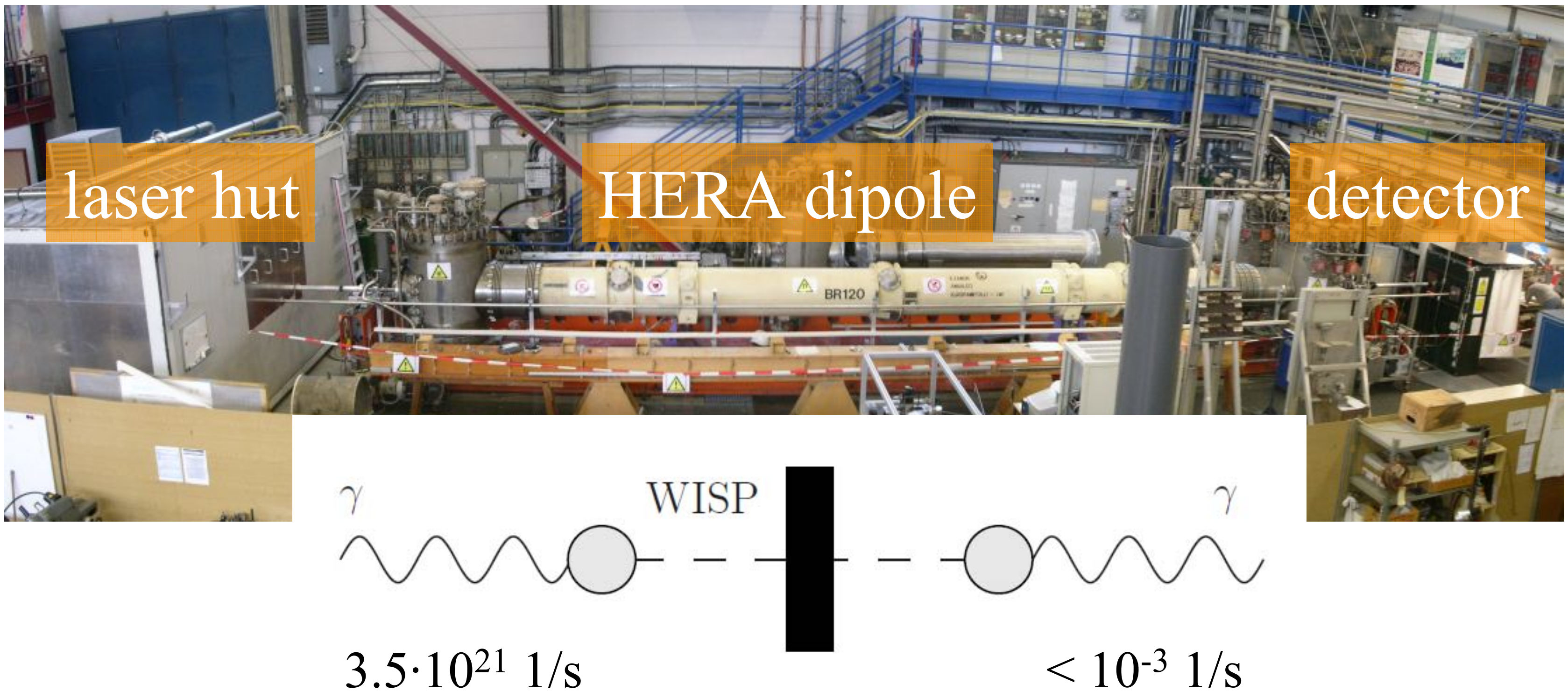

Light Shining through a Wall Experiments: ALPS

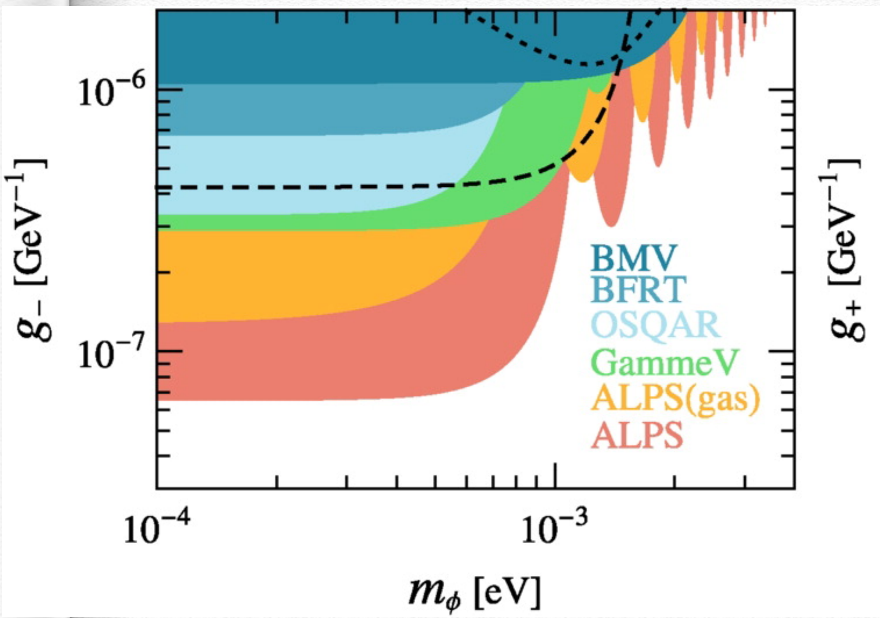

Ex: ALPS Desy use the Hera dipoles
N~ 10^{19} photons/s

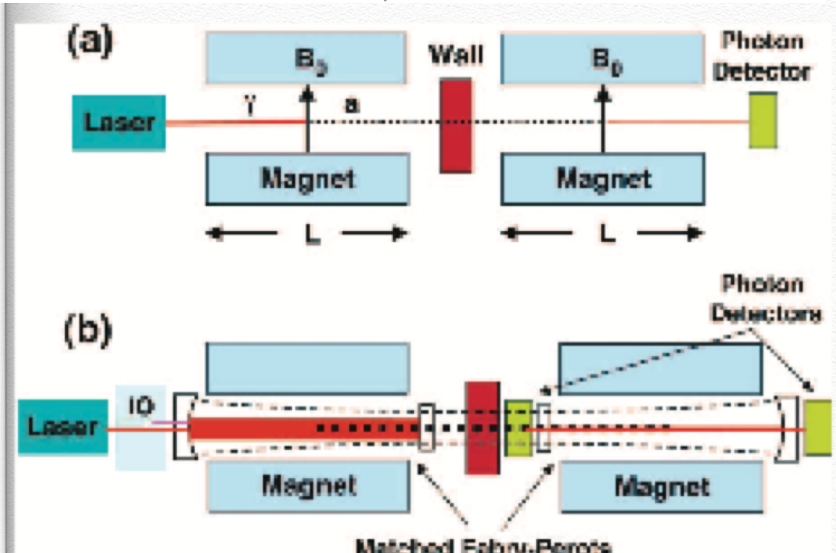

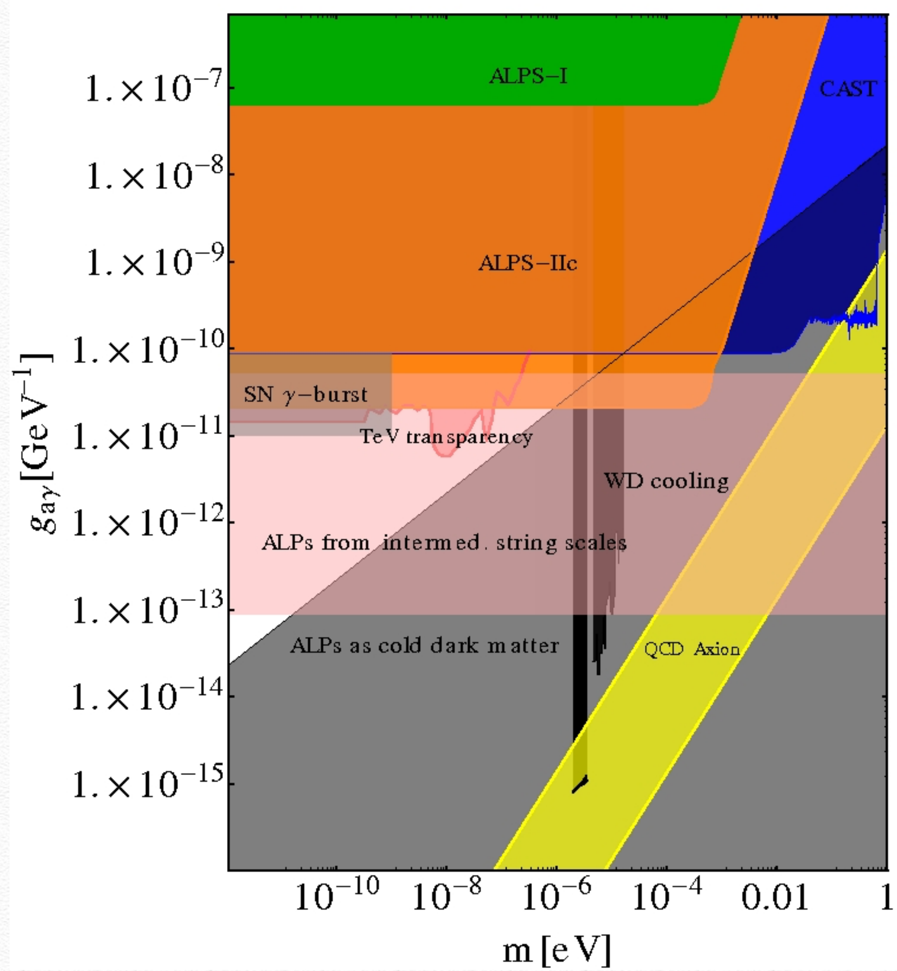

Light Shining through a Wall Experiments

P. Sikivie, Phys. Rev. Lett. **51**, 1415 (1983)

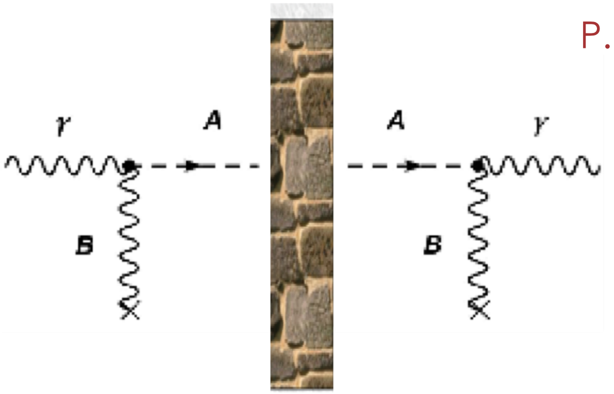

LAB experiment
Laser Source
Higher Luminosity

Double process
Rate ~ G^4

$$\dot{N}_{\text{evts}} \propto \dot{N}_\gamma\, P_{\gamma\to a} \times P_{a\to\gamma} \sim \dot{N}_\gamma\, G^4 H^4 L^4$$

Sensitivity on G linear with L and H, quartic root of luminosity (not depending on E_γ)

The NEXT key points are:

- High Luminosity (gyrotrons in the SubTHz region)
- intense H ~ 11 Tesla with L ~ 150 cm dipole
- Sub-THz single photon detector using TES

Optimal Working Point ~ 30 GHz

High Luminosity Photon Sources

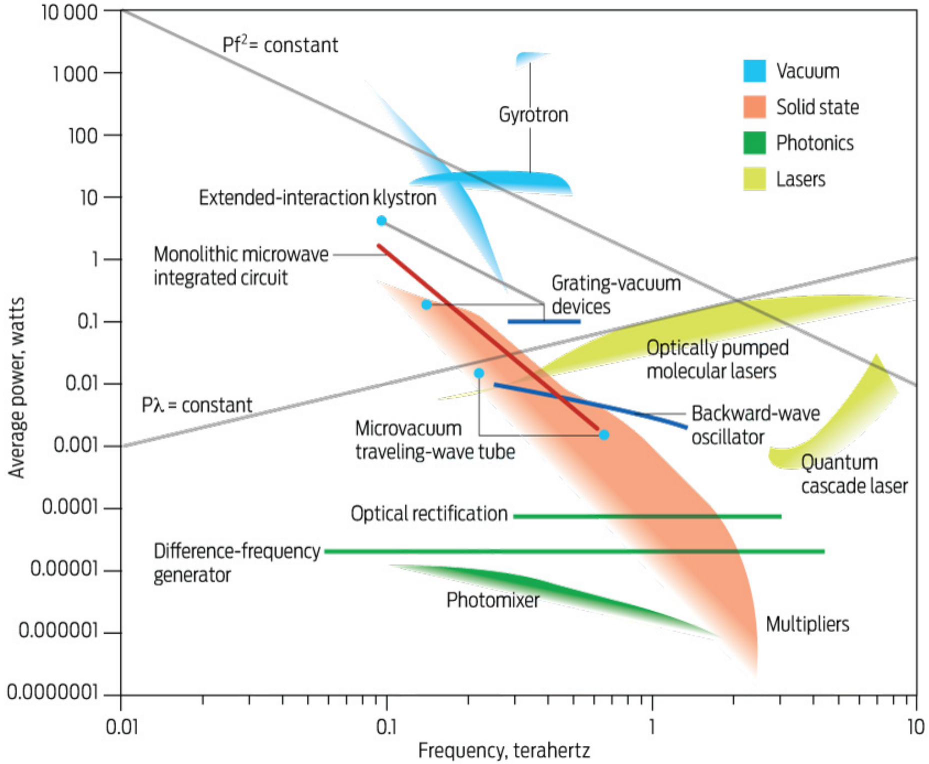

photon-axion conversion probability depends on luminosity, not energy
$\Rightarrow$ sub-THz

Reference:
30GHz ~120μeV ~ 1cm wave-length
Micro-waves domain

- Klystrons and gyrotrons sources in the 30-100 GHz range.
- Power exceeding 1 MW in this frequency range
- Luminosity up to 10^{28}-10^{29} γ/s in CW
- Lasers commonly used in LSW experiments ~ 10^{21} γ/s

Gyrotrons

$P(\text{MW}) \times \nu^2(\text{GHz}^2) = \text{const.}$

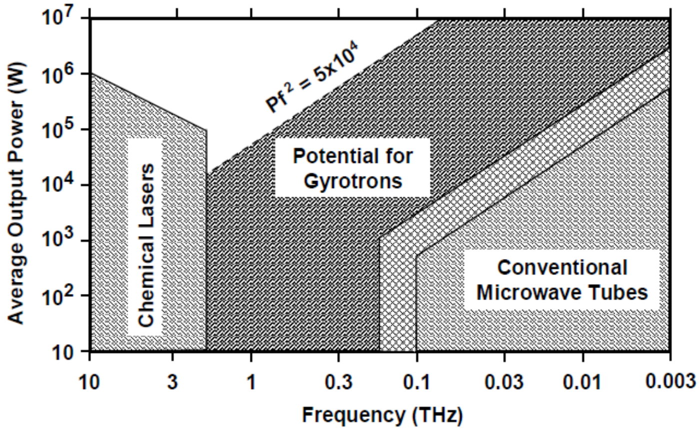

The operating region of gyrotrons

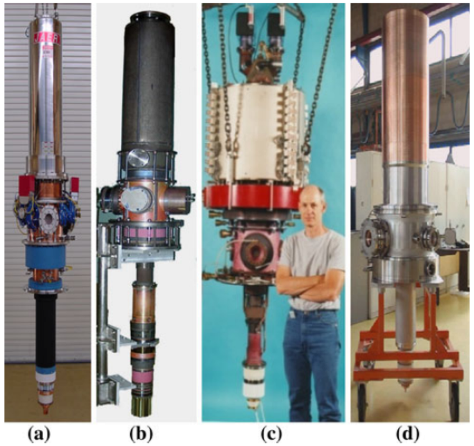

Fig. 2 Typical high power gyrotrons **a** JAERI/TOSHIBA 0.82 MW, 170 GHz, **b** GYCOM 1 MW, 170 GHz, **c** CPI 0.9 MW, 140 GHz, **d** TED 0.9 MW, 140 GHz

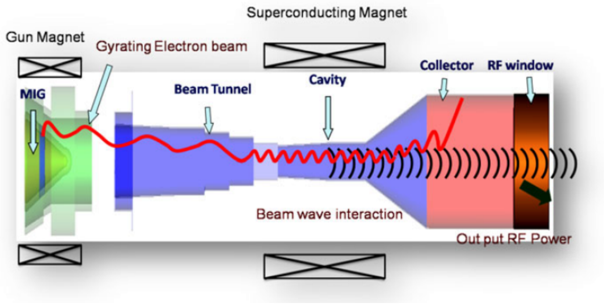

Now beyond 1 MW power

High-Power Cyclotron Autoresonance Maser (CARM)
Up to 10-15 MW with 10-50 GHz

STAX Experiment

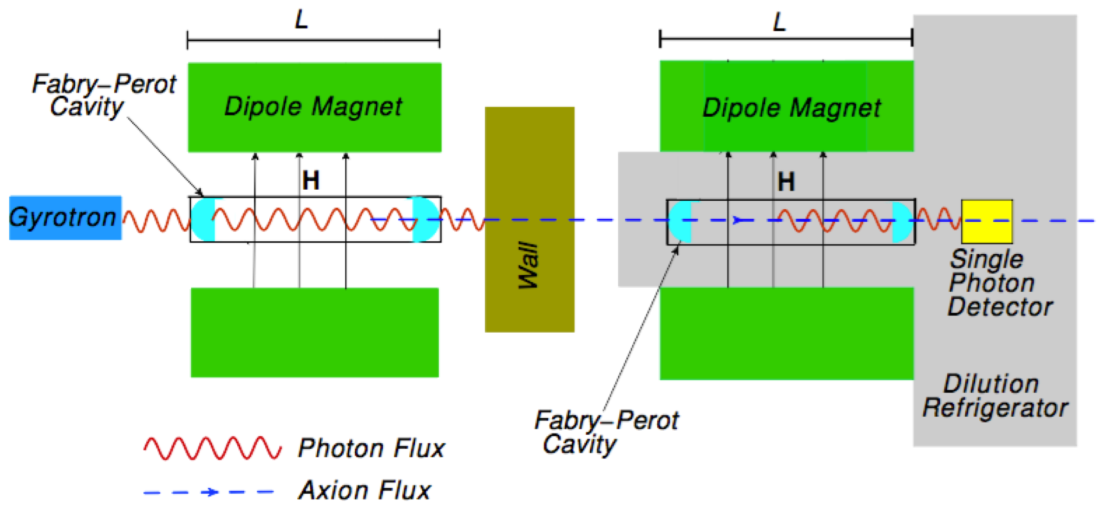

- Magnetic field: H = 11 T, L = 1.5 m
- Source: gyrotron; $P \approx 100$ kW, $\Phi_\gamma = 10^{27}$ s^{-1}, $\varepsilon_\gamma = 120$ µeV ($\nu \approx 30$ GHz)
- Fabry-Perot cavity: finesse $Q \approx 10^4$

- Sub-THz single-photon detection based on TES technology, $\eta \approx 1$
- Possible second FP cavity behind the wall to enhance axion-photon conversion rate

P. Sikivie, D.B. Tanner and K. Van Bibber, Phys. Rev. Lett. 98, 172002 (2007)

STAX detector

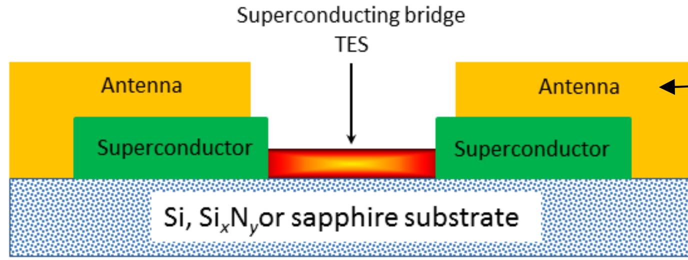

- Sub-THz single photon detector
- Transition Edge Sensor TES: ultra-low critical temperature superconductor bridge between two superconducting electrodes. TES coupled to a log periodic antenna.
- TES operates within its superconducting transition. DC bias voltage applied. When TES absorbs an incoming photon, it heats up above critical temperature Tc. Change of resistance and current flowing in the circuit, measured by a SQUID
- Material: choice of a Superconductor with low critical temperature ($T_c \approx 20$ mK) to have a good energy resolution α-W or bilayer Ti-Au or Ti-Cu
- TES bridge Ti-Cu (gap ~20 μeV), superconducting electrodes Nb (gap ~ 1 meV)
- Very high efficiency
- Ultra low background/dark count

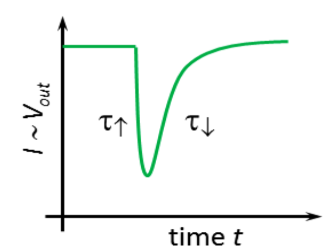

STAX detector

- Tailoring TES active volume to reduce thermal capacitance **(V ~10^{-3}-10^{-4} μm^3)**

$$\sigma_E \approx 0.3\sqrt{k_B T_c^2 C_e}$$

C = γ V T   V ~ 300x40x20 nm ^{3}

- low-noise SQUID readout electronics optimization (operating at 80 mK)
- Sensitivity $\delta T = \delta E / C_e$ thermalization $T(t) = \exp(-t/\tau)$ $\tau = C_e / G$
- σ(E)/E ~ 2% for 30 GHz photons

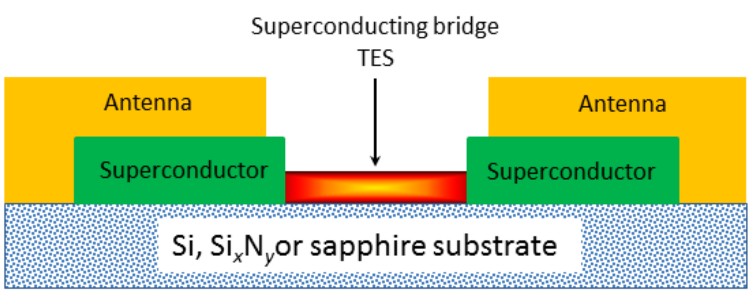

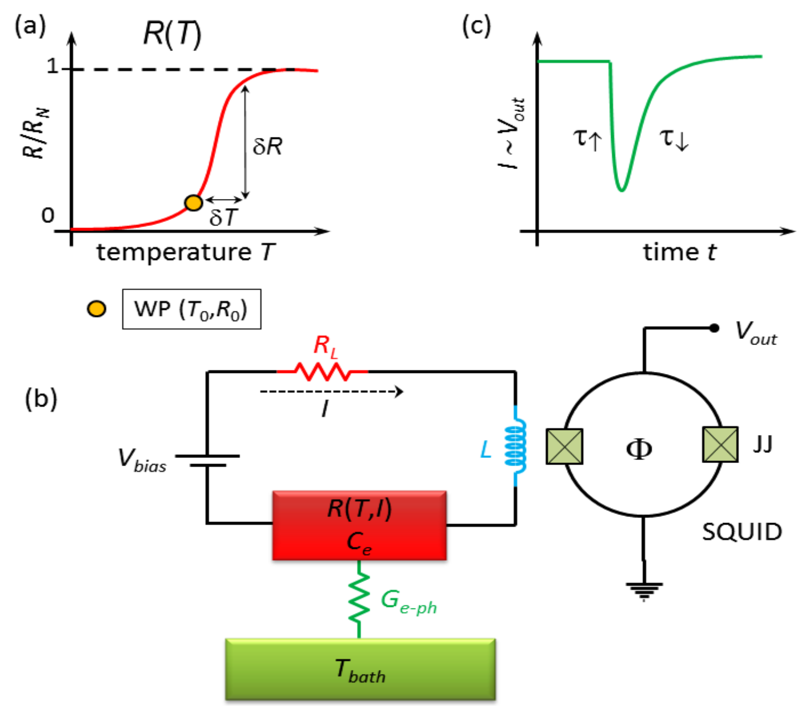

Noise

- Dark count rate (phonon noise) < 6x10 $^{-10}$ s^{-1}
- Black Body: at 10mK peaked around 0.6 GHz with a negligible rate of 10 $^{-30}$ m^{-2} s^{-1} photons irradiated
- Cosmic bkg: 1μ/cm^{-2}/min with 10 eV released in 10nm of material saturates the TES, bkg. under control translated in a negligible dead time of the TES ~ 0.1%

$$N_d = \frac{\beta_{eff}}{\sqrt{2\pi}} \int_{E_T/\sigma_E}^{\infty} exp(-x^2/2)\,\mathrm{d}x.$$

where $\beta_{eff} = 1/\tau_{eff}$ is the effective detection bandwidth, and E_T is the discrimination threshold energy.

$$\eta = \frac{1}{\sqrt{2\pi}} \int_{(E_T - h\nu)/\sigma_E}^{\infty} exp(-x^2/2)\,\mathrm{d}x.$$

11T dipole magnet

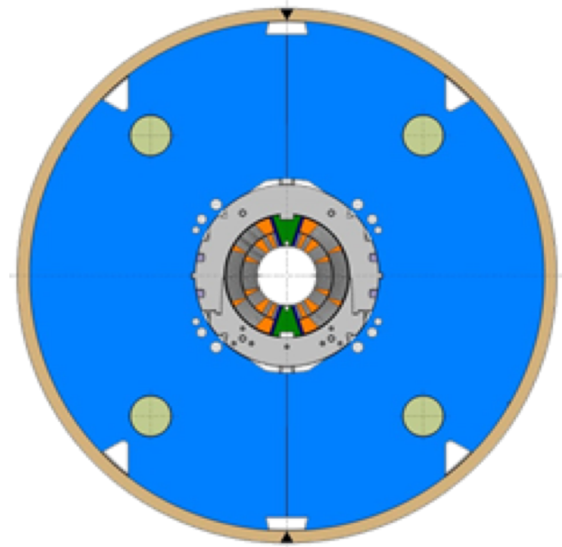

- The **HL-LHC Project** implies beams of larger intensity
  - Additional collimators are needed
- Two collimators to be installed on either side of interaction point 7
  - Replace a standard Main Dipole by a pair of shorter **11 T Dipoles**
- 5 single aperture **short models** fabricated and tested by CERN TE-MSC team
  - Bore field ranging from **10 to 12 T**
  - **60 mm** coil aperture
  - **~1.5 m** magnetic length

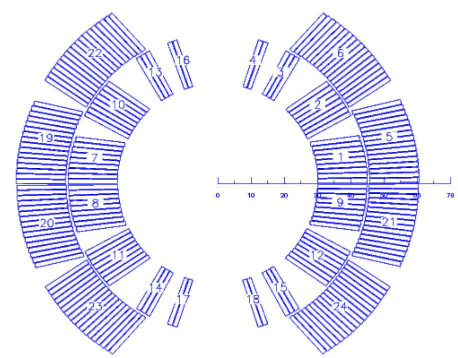

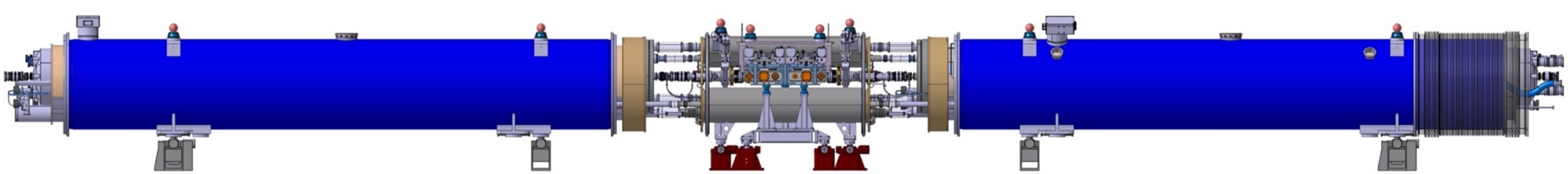

11T dipole magnet

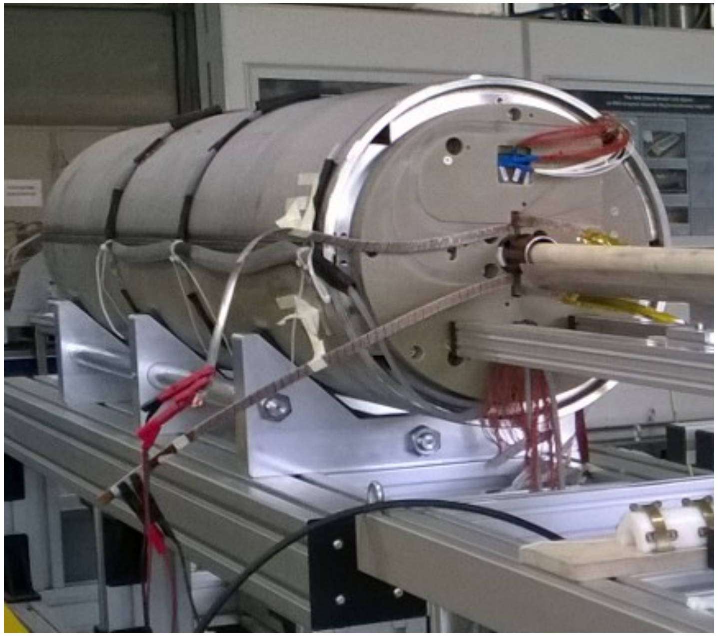
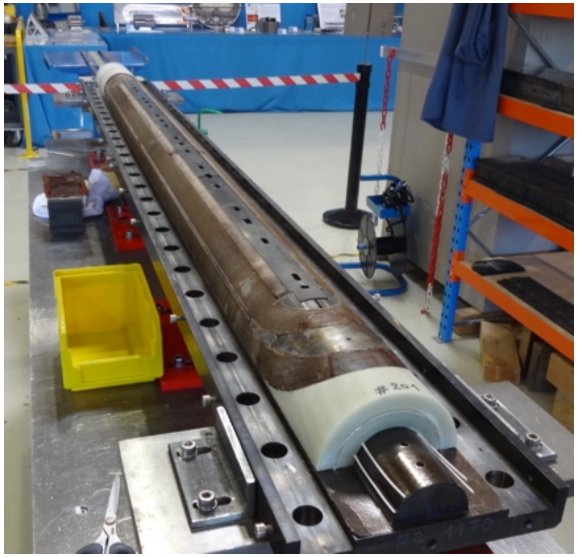
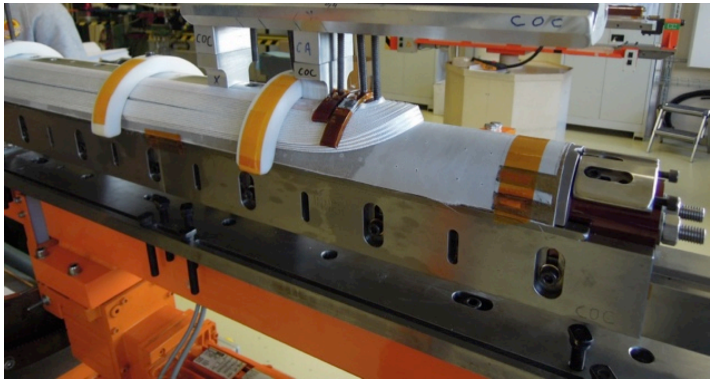
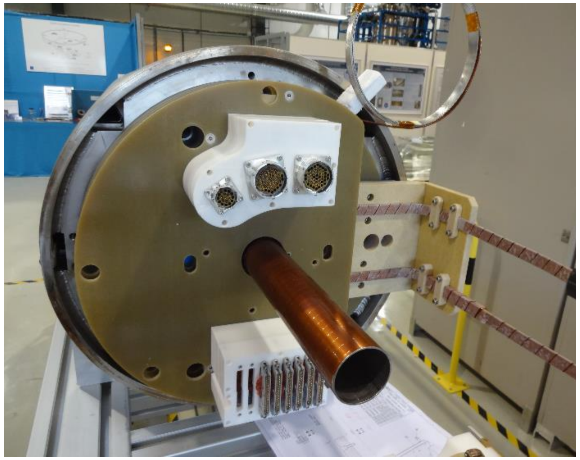

Constraints on $g_{A\gamma\gamma}$ vs. m_A